EUROPEAN LABORATORY FOR PARTICLE PHYSICS

CERN-EP/98-001
16th January 1998

Investigation of CP violation in $B^0 \to J/\psi K^0_S$ decays at LEP

The OPAL Collaboration

Abstract

An investigation of CP violation was performed using a total of 24 candidates for $B^0 \to J/\psi K^0_S$ decay, with a purity of about 60%. These events were selected from 4.4 million hadronic Z^0 decays recorded by the OPAL detector at LEP. An analysis procedure, involving techniques to reconstruct the proper decay times and tag the produced b-flavours, B^0 or $\bar{B}^0$, has been developed to allow a first direct study of the time dependent CP asymmetry that, in the Standard Model, is $\sin 2\beta$. The result is

$$\sin 2\beta = 3.2^{+1.8}_{-2.0} \pm 0.5 \ ,$$

where the first error is statistical and the second systematic. This result is used to determine probabilities for different values of $\sin 2\beta$ in the physical region from -1 to $+1$.

(Submitted to Physics Letters B)

The OPAL Collaboration

K. Ackerstaff[8], G. Alexander[23], J. Allison[16], N. Altekamp[5], K.J. Anderson[9], S. Anderson[12], S. Arcelli[2], S. Asai[24], S.F. Ashby[1], D. Axen[29], G. Azuelos[18,a], A.H. Ball[17], E. Barberio[8], R.J. Barlow[16], R. Bartoldus[3], J.R. Batley[5], S. Baumann[3], J. Bechtluft[14], T. Behnke[8], K.W. Bell[20], G. Bella[23], S. Bentvelsen[8], S. Bethke[14], S. Betts[15], O. Biebel[14], A. Biguzzi[5], S.D. Bird[16], V. Blobel[27], I.J. Bloodworth[1], M. Bobinski[10], P. Bock[11], D. Bonacorsi[2], M. Boutemeur[34], S. Braibant[8], L. Brigliadori[2], R.M. Brown[20], H.J. Burckhart[8], C. Burgard[8], R. Bürgin[10], P. Capiluppi[2], R.K. Carnegie[6], A.A. Carter[13], J.R. Carter[5], C.Y. Chang[17], D.G. Charlton[1,b], D. Chrisman[4], P.E.L. Clarke[15], I. Cohen[23], J.E. Conboy[15], O.C. Cooke[8], C. Couyoumtzelis[13], R.L. Coxe[9], M. Cuffiani[2], S. Dado[22], C. Dallapiccola[17], G.M. Dallavalle[2], R. Davis[30], S. De Jong[12], L.A. del Pozo[4], A. de Roeck[8], K. Desch[8], B. Dienes[33,d], M.S. Dixit[7], M. Doucet[18], E. Duchovni[26], G. Duckeck[34], I.P. Duerdoth[16], D. Eatough[16], P.G. Estabrooks[6], E. Etzion[23], H.G. Evans[9], M. Evans[13], F. Fabbri[2], A. Fanfani[2], M. Fanti[2], A.A. Faust[30], L. Feld[8], F. Fiedler[27], M. Fierro[2], H.M. Fischer[3], I. Fleck[8], R. Folman[26], D.G. Fong[17], M. Foucher[17], A. Fürtjes[8], D.I. Futyan[16], P. Gagnon[7], J.W. Gary[4], J. Gascon[18], S.M. Gascon-Shotkin[17], N.I. Geddes[20], C. Geich-Gimbel[3], T. Geralis[20], G. Giacomelli[2], P. Giacomelli[4], R. Giacomelli[2], V. Gibson[5], W.R. Gibson[13], D.M. Gingrich[30,a], D. Glenzinski[9], J. Goldberg[22], M.J. Goodrick[5], W. Gorn[4], C. Grandi[2], E. Gross[26], J. Grunhaus[23], M. Gruwé[27], C. Hajdu[32], G.G. Hanson[12], M. Hansroul[8], M. Hapke[13], C.K. Hargrove[7], P.A. Hart[9], C. Hartmann[3], M. Hauschild[8], C.M. Hawkes[5], R. Hawkings[27], R.J. Hemingway[6], M. Herndon[17], G. Herten[10], R.D. Heuer[8], M.D. Hildreth[8], J.C. Hill[5], S.J. Hillier[1], P.R. Hobson[25], A. Hocker[9], R.J. Homer[1], A.K. Honma[28,a], D. Horváth[32,c], K.R. Hossain[30], R. Howard[29], P. Hüntemeyer[27], D.E. Hutchcroft[5], P. Igo-Kemenes[11], D.C. Imrie[25], K. Ishii[24], A. Jawahery[17], P.W. Jeffreys[20], H. Jeremie[18], M. Jimack[1], A. Joly[18], C.R. Jones[5], M. Jones[6], U. Jost[11], P. Jovanovic[1], T.R. Junk[8], J. Kanzaki[24], D. Karlen[6], V. Kartvelishvili[16], K. Kawagoe[24], T. Kawamoto[24], P.I. Kayal[30], R.K. Keeler[28], R.G. Kellogg[17], B.W. Kennedy[20], J. Kirk[29], A. Klier[26], S. Kluth[8], T. Kobayashi[24], M. Kobel[10], D.S. Koetke[6], T.P. Kokott[3], M. Kolrep[10], S. Komamiya[24], R.V. Kowalewski[28], T. Kress[11], P. Krieger[6], J. von Krogh[11], P. Kyberd[13], G.D. Lafferty[16], R. Lahmann[17], W.P. Lai[19], D. Lanske[14], J. Lauber[15], S.R. Lautenschlager[31], I. Lawson[28], J.G. Layter[4], D. Lazic[22], A.M. Lee[31], E. Lefebvre[18], D. Lellouch[26], J. Letts[12], L. Levinson[26], B. List[8], S.L. Lloyd[13], F.K. Loebinger[16], G.D. Long[28], M.J. Losty[7], J. Ludwig[10], D. Lui[12], A. Macchiolo[2], A. Macpherson[30], M. Mannelli[8], S. Marcellini[2], C. Markopoulos[13], C. Markus[3], A.J. Martin[13], J.P. Martin[18], G. Martinez[17], T. Mashimo[24], P. Mättig[26], W.J. McDonald[30], J. McKenna[29], E.A. Mckigney[15], T.J. McMahon[1], R.A. McPherson[28], F. Meijers[8], S. Menke[3], F.S. Merritt[9], H. Mes[7], J. Meyer[27], A. Michelini[2], S. Mihara[24], G. Mikenberg[26], D.J. Miller[15], A. Mincer[22,e], R. Mir[26], W. Mohr[10], A. Montanari[2], T. Mori[24], S. Mihara[24], K. Nagai[26], I. Nakamura[24], H.A. Neal[12], B. Nellen[3], R. Nisius[8], S.W. O'Neale[1], F.G. Oakham[7], F. Odorici[2], H.O. Ogren[12], A. Oh[27], N.J. Oldershaw[16], M.J. Oreglia[9], S. Orito[24], J. Pálinkás[33,d], G. Pásztor[32], J.R. Pater[16], G.N. Patrick[20], J. Patt[10], R. Perez-Ochoa[8], S. Petzold[27], P. Pfeifenschneider[14], J.E. Pilcher[9], J. Pinfold[30], D.E. Plane[8], P. Poffenberger[28], B. Poli[2], A. Posthaus[3], C. Rembser[8], S. Robertson[28], S.A. Robins[22], N. Rodning[30], J.M. Roney[28], A. Rooke[15], A.M. Rossi[2], P. Routenburg[30], Y. Rozen[22], K. Runge[10], O. Runolfsson[8], U. Ruppel[14], D.R. Rust[12], K. Sachs[10], T. Saeki[24], O. Sahr[34], W.M. Sang[25], E.K.G. Sarkisyan[23], C. Sbarra[29], A.D. Schaile[34], O. Schaile[34], F. Scharf[3], P. Scharff-Hansen[8], J. Schieck[11], P. Schleper[11], B. Schmitt[8], S. Schmitt[11], A. Schöning[8], M. Schröder[8], M. Schumacher[3], C. Schwick[8], W.G. Scott[20], T.G. Shears[8], B.C. Shen[4], C.H. Shepherd-Themistocleous[8],

P. Sherwood[15], G.P. Siroli[2], A. Sittler[27], A. Skillman[15], A. Skuja[17], A.M. Smith[8], G.A. Snow[17], R. Sobie[28], S. Söldner-Rembold[10], R.W. Springer[30], M. Sproston[20], K. Stephens[16], J. Steuerer[27], B. Stockhausen[3], K. Stoll[10], D. Strom[19], R. Ströhmer[34], P. Szymanski[20], R. Tafirout[18], S.D. Talbot[1], P. Taras[18], S. Tarem[22], R. Teuscher[8], M. Thiergen[10], M.A. Thomson[8], E. von Törne[3], E. Torrence[8], S. Towers[6], I. Trigger[18], Z. Trócsányi[33], E. Tsur[23], A.S. Turcot[9], M.F. Turner-Watson[8], I. Ueda[24], P. Utzat[11], R. Van Kooten[12], P. Vannerem[10], M. Verzocchi[10], P. Vikas[18], E.H. Vokurka[16], H. Voss[3], F. Wäckerle[10], A. Wagner[27], C.P. Ward[5], D.R. Ward[5], P.M. Watkins[1], A.T. Watson[1], N.K. Watson[1], P.S. Wells[8], N. Wermes[3], J.S. White[28], G.W. Wilson[27], J.A. Wilson[1], T.R. Wyatt[16], S. Yamashita[24], G. Yekutieli[26], V. Zacek[18], D. Zer-Zion[8]

[1]School of Physics and Astronomy, University of Birmingham, Birmingham B15 2TT, UK
[2]Dipartimento di Fisica dell' Università di Bologna and INFN, I-40126 Bologna, Italy
[3]Physikalisches Institut, Universität Bonn, D-53115 Bonn, Germany
[4]Department of Physics, University of California, Riverside CA 92521, USA
[5]Cavendish Laboratory, Cambridge CB3 0HE, UK
[6]Ottawa-Carleton Institute for Physics, Department of Physics, Carleton University, Ottawa, Ontario K1S 5B6, Canada
[7]Centre for Research in Particle Physics, Carleton University, Ottawa, Ontario K1S 5B6, Canada
[8]CERN, European Organisation for Particle Physics, CH-1211 Geneva 23, Switzerland
[9]Enrico Fermi Institute and Department of Physics, University of Chicago, Chicago IL 60637, USA
[10]Fakultät für Physik, Albert Ludwigs Universität, D-79104 Freiburg, Germany
[11]Physikalisches Institut, Universität Heidelberg, D-69120 Heidelberg, Germany
[12]Indiana University, Department of Physics, Swain Hall West 117, Bloomington IN 47405, USA
[13]Queen Mary and Westfield College, University of London, London E1 4NS, UK
[14]Technische Hochschule Aachen, III Physikalisches Institut, Sommerfeldstrasse 26-28, D-52056 Aachen, Germany
[15]University College London, London WC1E 6BT, UK
[16]Department of Physics, Schuster Laboratory, The University, Manchester M13 9PL, UK
[17]Department of Physics, University of Maryland, College Park, MD 20742, USA
[18]Laboratoire de Physique Nucléaire, Université de Montréal, Montréal, Quebec H3C 3J7, Canada
[19]University of Oregon, Department of Physics, Eugene OR 97403, USA
[20]Rutherford Appleton Laboratory, Chilton, Didcot, Oxfordshire OX11 0QX, UK
[22]Department of Physics, Technion-Israel Institute of Technology, Haifa 32000, Israel
[23]Department of Physics and Astronomy, Tel Aviv University, Tel Aviv 69978, Israel
[24]International Centre for Elementary Particle Physics and Department of Physics, University of Tokyo, Tokyo 113, and Kobe University, Kobe 657, Japan
[25]Institute of Physical and Environmental Sciences, Brunel University, Uxbridge, Middlesex UB8 3PH, UK
[26]Particle Physics Department, Weizmann Institute of Science, Rehovot 76100, Israel
[27]Universität Hamburg/DESY, II Institut für Experimental Physik, Notkestrasse 85, D-22607 Hamburg, Germany

[28]University of Victoria, Department of Physics, P O Box 3055, Victoria BC V8W 3P6, Canada
[29]University of British Columbia, Department of Physics, Vancouver BC V6T 1Z1, Canada
[30]University of Alberta, Department of Physics, Edmonton AB T6G 2J1, Canada
[31]Duke University, Dept of Physics, Durham, NC 27708-0305, USA
[32]Research Institute for Particle and Nuclear Physics, H-1525 Budapest, P O Box 49, Hungary
[33]Institute of Nuclear Research, H-4001 Debrecen, P O Box 51, Hungary
[34]Ludwigs-Maximilians-Universität München, Sektion Physik, Am Coulombwall 1, D-85748 Garching, Germany

[a] and at TRIUMF, Vancouver, Canada V6T 2A3
[b] and Royal Society University Research Fellow
[c] and Institute of Nuclear Research, Debrecen, Hungary
[d] and Department of Experimental Physics, Lajos Kossuth University, Debrecen, Hungary
[e] and Department of Physics, New York University, NY 1003, USA

1 Introduction

CP violation was observed in 1964 in K^0 decays [1], and, so far, this phenomenon has been seen only in the K system. CP violation can be accommodated in the Standard Model, provided that the CKM matrix elements are allowed to be complex. The CP violating effects associated with b hadrons are expected to be larger than in the K system [2]. It is therefore important to investigate CP violation in the B system, where the relation between CKM matrix elements and CP violation can be tested. Previous studies, yielding null results [3, 4], have focussed on CP violation in inclusive B decays, predicted to be at the level of 10^{-3}.

This paper presents a study of CP violation in $B^0 \to J/\psi K^0_S$ decays. The decay mode $J/\psi K^0_S$ has long been considered a 'golden' channel for CP violation studies [2, 5], since the final state is a CP eigenstate which is experimentally favourable for reconstruction because the J/ψ and K^0_S are narrow states and $J/\psi \to \ell^+\ell^-$ decays give a distinctive signature. In addition, CP violation in this channel is dominated by diagrams having a single relative phase, allowing a clean extraction of the phase of a CKM matrix element. In the Standard Model, the expected time-dependent rate asymmetry, $A(t)$, is given by

$$A(t) \equiv \frac{B^0(t) - \bar{B}^0(t)}{B^0(t) + \bar{B}^0(t)} = -\sin 2\beta \sin \Delta m_d t \ , \tag{1}$$

where the parameter Δm_d is the mass difference between the two B^0 mass eigenstates and $B^0(t)$ ($\bar{B}^0(t)$) represents the rate of produced B^0's ($\bar{B}^0$'s) decaying to $J/\psi K^0_S$ at a given proper decay time, t. The angle β is given by

$$\beta \equiv \arg\left[\frac{V_{td}V^*_{tb}}{V_{cd}V^*_{cb}}\right] \approx -\arg V_{td} \ . \tag{2}$$

Constraints on the CKM matrix, including measurements of CP violation in the K system, imply that the Standard Model expectation for $\sin 2\beta$ lies in the range 0.3–0.9 [2]. Other models of CP violation, such as the Superweak model [6], would give a time dependence of the same form, but with $\sin 2\beta$ replaced by another amplitude of magnitude less than or equal to one.

At LEP, due to the small branching ratios of $B^0 \to J/\psi K^0_S$ and $J/\psi \to \ell^+\ell^-$, only a handful of these decays may be seen. It is therefore important to maximise the reconstruction efficiency and to determine the b-flavour at production with a minimum error rate. In contrast, the proper time resolution is not critical, since the frequency of B^0 oscillation is easily resolved. In this analysis, $B^0 \to J/\psi K^0_S$ decays are reconstructed and their decay proper times are measured. The production flavour (B^0 or $\bar{B}^0$) of each candidate is determined using a combination of jet and vertex charge techniques. The CP-violating amplitude, $\sin 2\beta$, is extracted using an unbinned maximum likelihood fit to the proper-time distribution of the selected data. Such a fit has higher expected sensitivity than a time-integrated fit, even if the domain of integration of the latter is optimised, since it uses the additional, well measured, decay-time information.

The next section describes the event selection and proper time estimation. Section 3 describes the tagging of the production flavour. In section 4, the fits and results are presented, with systematic errors discussed in section 5. Discussion of the result and conclusions are given in section 6.

2 $B^0 \to J/\psi K^0_S$ reconstruction

A detailed description of the OPAL detector may be found elsewhere [7]. The basic selection of $B^0 \to J/\psi K^0_S$ decays was described in a previous publication [8], which used data collected between 1990 and 1994 to identify various exclusive B decay modes. For this analysis, the 1995 data were included to give a total of 4.4 million events passing the basic hadronic event selection. The efficiency of the $B^0 \to J/\psi K^0_S$ selection was also improved (and applied to the full data sample) by relaxing or modifying the criteria, at the expense of a somewhat larger background. The efficiency and purity of the selection was studied using Monte Carlo events generated with Jetset 7.4 [9] and processed through the OPAL detector simulation [10].

Lepton candidates were required to satisfy the polar angle[1] cut $|\cos\theta| < 0.97$ and to have track momenta larger than 1.5 GeV/c (2 GeV/c) for muon (electron) candidates. Muons were identified by requiring an extrapolated track to match the position of a muon chamber segment to within 4 standard deviations. Muon candidates were also considered if the muon chamber segment had no z-coordinate reconstructed, provided that the matching in position and angle were within 4 standard deviations in the r-ϕ plane. As in [8], muons identified in the hadronic calorimeter were accepted in regions without muon chamber coverage.

Electrons were identified [11] and photon conversions rejected [12] using artificial neural network algorithms. When the electron energies are determined only from the reconstructed track momenta, photon radiation causes the reconstructed J/ψ mass spectrum to have a long tail to lower masses, reducing the efficiency of a mass cut. Therefore the electron energies were determined using in addition the information from the lead-glass calorimeter. The energy contained in a cone of 30 mrad around the impact point of the electron track on the calorimeter, plus energy contained in lead-glass blocks touching this cone, were summed [13]. This sum was used as the energy of the electron if larger than the track momentum, otherwise the track momentum was used.

J/ψ candidates were selected by demanding two electron or two muon candidates of opposite charge with an opening angle of less than 90°. The invariant mass of the two leptons was required to lie in the range 2.95–3.25 GeV/c^2 for $J/\psi \to \mu^+\mu^-$ candidates and 2.95–3.40 GeV/c^2 for $J/\psi \to e^+e^-$ candidates (in the latter case over-correction for photon radiation causes a significant tail at higher masses).

The K^0_S selection was based on the procedure described previously [15], considering the intersection of all track pairs of opposite charge (excepting J/ψ candidate tracks) passing certain quality criteria. The projection of the the K^0_S momentum vector in the r-ϕ plane was required to point back to the beam spot position to within 8°. The beam spot position was measured using charged tracks from many consecutive events, thus following any significant shifts in beam position during a LEP fill [16]. The impact parameter[2] significance (the impact parameter divided by its error) in the r-ϕ plane of the K^0_S with respect to the J/ψ vertex was required to be less than 5. The reconstructed distance between the J/ψ vertex and the K^0_S decay vertex,

[1] The right-handed coordinate system is defined with positive z along the e^- beam direction, x pointing to the centre of the LEP ring, θ and ϕ as the polar and azimuthal angles, and $r^2 = x^2 + y^2$. The origin is taken to be the centre of the detector.

[2] The impact parameter of a track with respect to a vertex is defined as the distance of closest approach of the track to that vertex.

divided by its error, was required to exceed 2. If the K^0_S decay vertex was inside the active volume of the jet chamber ($r > 30\,\mathrm{cm}$), the radial coordinate of the first jet chamber hit on either track was required to be at most 10 cm less than the decay vertex radial coordinate, and the tracks were required not to have any associated vertex chamber or silicon microvertex detector hits. The invariant mass of the K^0_S candidate was required to lie in the range 0.45–0.55 GeV/c^2. In order to suppress a potential background from $\Lambda_b \to J/\psi\Lambda$ decays, the K^0_S candidate was rejected if its invariant mass under either proton-pion hypothesis was in the range 1.110–1.121 GeV/c^2.

B^0 candidates were reconstructed by combining J/ψ and K^0_S candidates from the same thrust hemisphere[3]. Kinematic fitting using the SQUAW package [14], constraining the J/ψ and K^0_S masses to their nominal values, was employed, and the probability of the kinematic fit was required to exceed 1%. The invariant masses of selected B^0 candidates were required to lie in the range 5.0–5.6 GeV/c^2, and the B^0 energies to exceed 20 GeV. The efficiency for reconstructing the decay $B^0 \to J/\psi K^0_S \to \ell^+\ell^-\pi^+\pi^-$ was estimated to be $17.3 \pm 1.4\%$ where the error is due to Monte Carlo statistics. This compares to 10.9% for the previous selection [8].

The distribution of reconstructed mass is shown in Figure 1(a) for candidates passing the entire selection except the $J/\psi K^0_S$ mass cut. In total, 24 candidates were selected in the mass region 5.0–5.6 GeV/c^2. The background was estimated from the data using an unbinned maximum likelihood fit to the joint distribution of the $J/\psi K^0_S$ mass and energy, including mass values between 4 and 7 GeV/c^2. The shape of the mass distribution for the signal was taken from Monte Carlo, and parametrised using two Gaussians for the peak of the distribution and a third to account for a significant tail to lower masses. The shape of the background mass distribution was also taken from Monte Carlo, and parametrised using a polynomial function.

The mass and energy distributions were taken to be uncorrelated both for the signal and the background, since the correlations seen in Monte Carlo were small and had a negligible effect on the fit. Peterson fragmentation functions [17] were used to parametrise the energy distributions. For the signal, the Peterson parameter ϵ was taken from a fit to the Monte Carlo energy distribution, while for the background it was allowed to vary. In total, three parameters were allowed to vary in the fit: the number of signal candidates, the position of the B^0 mass peak and the Peterson parameter for the background energy distribution. The result of the fit is shown in Figure 1(a) as a function of mass, in Figure 1(b) as a function of energy for masses between 5.0 and 5.6 GeV/c^2 (signal region) and in Figure 1(c) as a function of energy for masses outside this region (sideband). The overall fitted purity of the 24 $B^0 \to J/\psi K^0_S$ candidates is $60 \pm 8\%$, where the error is statistical. The fit was used not only to determine the overall purity of the sample, but also to assign event-by-event background probabilities, f_{bac}, to be used in the fit for $\sin 2\beta$, according to the reconstructed $J/\psi K^0_S$ mass and energy of each candidate.

The B^0 decay length, l_{B^0}, was determined from the distance between the average beam spot position and the J/ψ vertex in the x-y projection, correcting for the polar angle using the direction of the $J/\psi K^0_S$ momentum vector. The B^0 momentum, p_{B^0}, was taken from the constrained fit of the $J/\psi K^0_S$ system, and the proper decay time was then calculated as

$$t_{\mathrm{rec}} = l_{B^0} \cdot \frac{M_{B^0}}{p_{B^0}} \,, \tag{3}$$

[3] The two hemispheres were separated by the plane perpendicular to the thrust axis of the event and containing the e^+e^- interaction point.

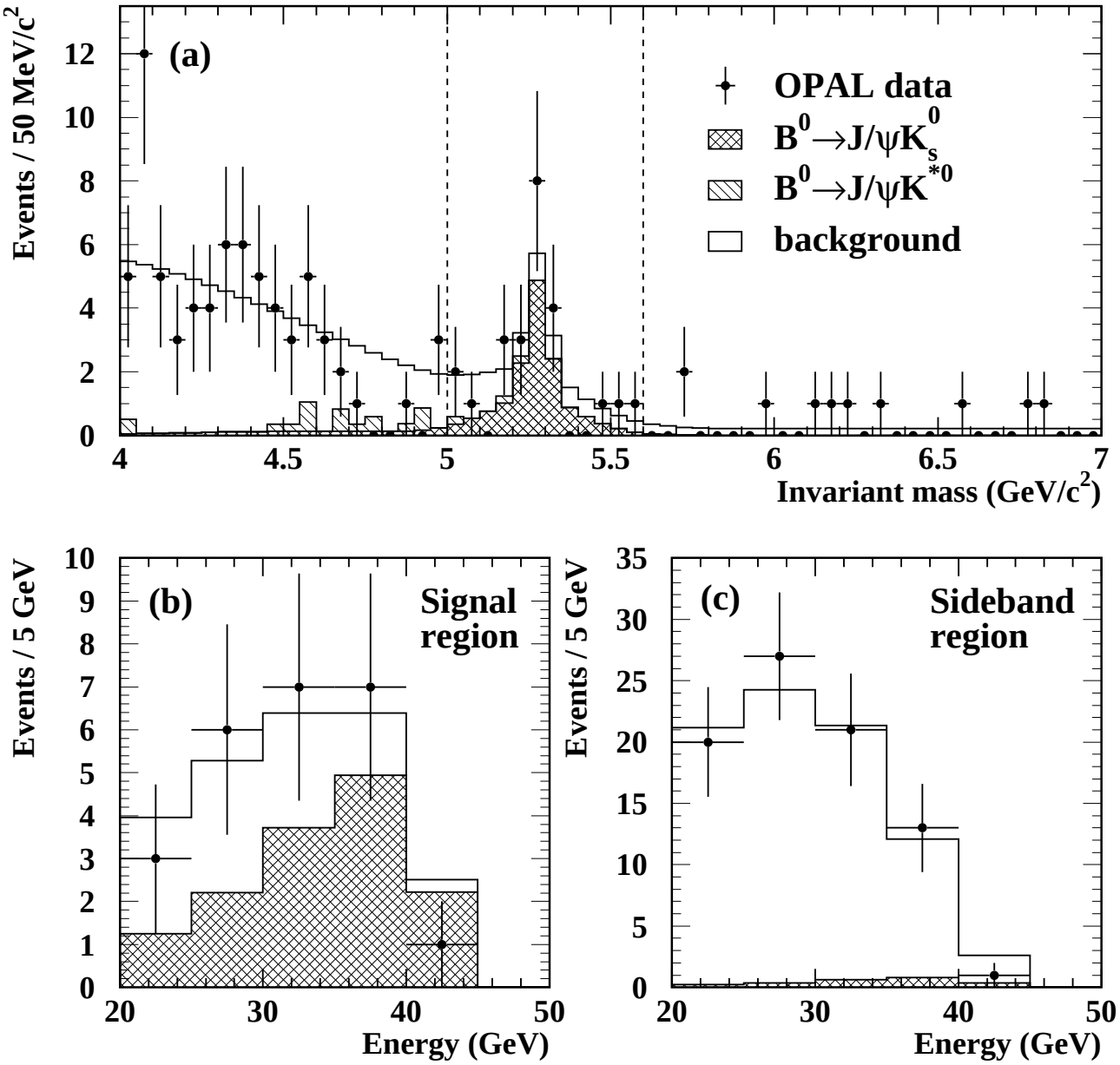

Figure 1: (a) The mass distribution of $J/\psi K^0_S$ candidates. (b) The energy distribution of the candidates with masses between 5.0 and 5.6 GeV/c^2. (c) The energy distribution of the candidates with masses outside this region. In each case, the data are shown by the points with error bars, and the fit is shown by the open histogram. The estimated contribution from the $B^0 \to J/\psi K^0_S$ signal is shown by the cross hatched histogram. The estimated contribution from $B^0 \to J/\psi K^{*0}$ is also shown in (a) by the hatched histogram. Note that the $J/\psi K^{*0}$ contribution is taken directly from Monte Carlo, while the shapes of the other distributions are parametrised (see text).

where M_{B^0} is the B^0 mass, taken to be $5.279\,\mathrm{GeV}/c^2$ [18]. The uncertainty on t_{rec}, typically $\sigma_t = 0.1\,\mathrm{ps}$, was estimated by combining the uncertainties on l_{B^0} and p_{B^0}.

3 Tagging the produced b-flavour

Information from the rest of the event was used to determine the production flavour of each candidate. The weighted track charge sum, or 'jet charge', gives information on the charge, and hence b-flavour, of the primary quark initiating the jet within which the $\mathrm{J}/\psi\mathrm{K}^0_{\mathrm{S}}$ candidate was isolated. Additionally, since the Z^0 decays into quark-antiquark pairs, measuring the b-flavour of the other b quark produced in the event also provides information on the production flavour.

In this analysis, three different pieces of information were used to determine the B^0 production flavour[4]: (a) the jet charge of the highest energy jet other than that containing the B^0 candidate, (b) the jet charge of the jet containing the B^0 candidate, excluding the tracks from the J/ψ and $\mathrm{K}^0_{\mathrm{S}}$ decays, and (c) the vertex charge of a significantly separated vertex (if existing) in the opposite hemisphere.

Jets were reconstructed from tracks and electromagnetic clusters not associated to tracks using the JADE E0 recombination scheme [19] with a y_{cut} value of 0.04.

The jet charge for the highest energy jet other than the one containing the $\mathrm{J}/\psi\mathrm{K}^0_{\mathrm{S}}$ candidate was calculated as :

$$Q_{\mathrm{opp}} = \sum_i \left(\frac{p_i^l}{E_{\mathrm{beam}}} \right)^{\kappa} q_i \ , \tag{4}$$

where p_i^l is the longitudinal component of the momentum of track i with respect to the jet axis, E_{beam} is the beam energy, q_i is the electric charge (± 1) of each track and the sum is taken over all tracks in the jet. Using simulated data, the value of κ that minimised the mistag probability (the probability to tag a B^0 as $\bar{\mathrm{B}}^0$ and vice versa), was found to be approximately 0.5. The mistag probability includes the effect of B^0 mixing in this jet. The jet charge for the jet containing the B^0 candidate, Q_{same}, was calculated in the same way, but excluding the J/ψ and $\mathrm{K}^0_{\mathrm{S}}$ decay products. These particles contain no information on whether their parent was produced as a B^0 or $\bar{\mathrm{B}}^0$, and would only dilute the information from the fragmentation tracks. The optimal value of κ was found to be 0.4 in this case, smaller than that for the other b-hadron as the high momentum B decay products were excluded.

Secondary vertices were reconstructed in jets in the hemisphere opposite to the B^0 candidate in data where silicon microvertex information was available, using the algorithm described in [20]. For the 1991 and 1992 data, vertices were reconstructed in the x-y plane only. In the 1993–1995 data, precise z coordinate information from the silicon microvertex detector was also available, and vertices were reconstructed in three dimensions using an extension of the vertex finding algorithm as in [21]. A secondary vertex was accepted if the distance from the primary to the secondary vertex divided by its error (the vertex significance) exceeded 3. If more than one vertex in the opposite hemisphere satisfied this requirement the one with the highest

[4] Leptons in the opposite hemisphere were also investigated as a possible tag, but in this sample the events with selected leptons were found to have large jet charges (in agreement with the lepton charge), so that there was no significant gain in tag purity from the use of leptons.

significance was taken. Approximately 40% of Monte Carlo $B^0 \to J/\psi K^0_S$ events had such an accepted secondary vertex in the opposite hemisphere. For the selected vertex, the charge $Q_{\rm vtx}$ and its uncertainty $\sigma_{Q{\rm vtx}}$ were calculated using an improved version of the algorithm described in [22]. For each track i in the jet containing the vertex, the track momentum, the momentum transverse to the jet axis, and the track impact parameters with respect to the primary and secondary vertices in the r-ϕ and r-z planes (the r-z information was only used in 1993–1995 data) were combined to form a weight w_i using an artificial neural network algorithm. The weight w_i quantifies the probability for track i to belong to the selected secondary vertex. The vertex charge is then calculated as:

$$Q_{\rm vtx} = \sum_i w_i q_i \ , \tag{5}$$

and the uncertainty as:

$$\sigma^2_{Q{\rm vtx}} = \sum_i w_i (1 - w_i) q_i^2 \ . \tag{6}$$

For events with such a selected secondary vertex (9 of the 24 B^0 candidates fall into this category), a neural network was constructed to tag the produced B^0 or $\bar{B}^0$, combining the four inputs, $Q_{\rm vtx}$, $\sigma_{Q{\rm vtx}}$, $Q^{\kappa=0.5}_{\rm opp}$ and $Q^{\kappa=0.4}_{\rm same}$. The network was trained on a large Monte Carlo sample, and a variable

$$Q_{\rm B}(x) = f_{\rm B^0}(x) - f_{\bar{\rm B}^0}(x) \tag{7}$$

was calculated as a function of the network output, x, where $f_{\rm B^0}(x)$ ($f_{\bar{\rm B}^0}(x)$) is the fraction of candidates at a particular value of x due to produced B^0 ($\bar{B}^0$) according to Monte Carlo (which included the effects of B^0 mixing). The variable $Q_{\rm B}$ represents the effective produced b-flavour for each candidate ($Q_{\rm B} = +1$ or -1 for pure B^0 or $\bar{B}^0$, respectively), and $|Q_{\rm B}| = 1 - 2\eta$ the tagging dilution, where η is the probability to tag the production flavour incorrectly. The average value of $|Q_{\rm B}|$ is 0.38 for such events, according to Monte Carlo.

For events without such a selected secondary vertex, only the jet charge information is available. In this case the two jet charges were combined linearly to form

$$Q_{\rm 2jet} = Q^{\kappa=0.4}_{\rm same} - 1.43 \cdot Q^{\kappa=0.5}_{\rm opp} \ , \tag{8}$$

where the factor of 1.43 was optimised using simulated data to minimise η. Distributions $f_{\rm B^0}(Q_{\rm 2jet})$ and $f_{\bar{\rm B}^0}(Q_{\rm 2jet})$ were formed and $Q_{\rm B}(Q_{\rm 2jet})$ was determined by analogy to equation 7. For these events, the Monte Carlo predicts the average value of $|Q_{\rm B}|$ to be 0.31.

It is important to ensure that the tagging dilution arising from the jet and vertex charges, which are used to determine the $Q_{\rm B}$ values, is correctly modelled by the Monte Carlo. The tagging dilutions arising from $Q^{\kappa=0.5}_{\rm opp}$ and from $Q_{\rm vtx}$ were checked using large samples of data and Monte Carlo inclusive lepton events, selected as in [4]. In such events, the charge of the lepton (usually from a semileptonic decay of a b hadron), is strongly correlated with the produced b-flavour. The distributions of $Q^{\kappa=0.5}_{\rm opp}$ and $Q_{\rm vtx}$, multiplied by the lepton charge Q_ℓ, were compared for data and Monte Carlo, and found to be consistent (see Figures 2(a) and (b)). The mean values of these distributions (which are sensitive to the tagging dilution of $Q^{\kappa=0.5}_{\rm opp}$ or $Q_{\rm vtx}$) for data divided by those in the Monte Carlo, were found to be 1.13 ± 0.09 and 1.05 ± 0.11 for $Q^{\kappa=0.5}_{\rm opp}$ and $Q_{\rm vtx}$ respectively. The $Q^{\kappa=0.4}_{\rm same}$ dilution was checked using samples of $B^0 \to D^{*\pm}\ell$ candidates selected in data and Monte Carlo, as in [23]. (In calculating $Q^{\kappa=0.4}_{\rm same}$, tracks from

the $D^{*\pm}\ell$ combinations were excluded.) The average dilution seen in the data divided by that observed in Monte Carlo was found to be 0.98 ± 0.20. The distributions of $Q_\ell \cdot Q^{\kappa=0.4}_{\rm same}$ for data and Monte Carlo are shown in Figure 2(c). Only events with reconstructed B^0 decay time $t_{\rm rec} < 2\,{\rm ps}$ are included, to reduce the tagging dilution due to B^0 mixing.

The samples of $D^{*\pm}\ell$ events were also used to check the tagging dilution of the $Q_{\rm B}$ values (formed from the combinations of jet and vertex charges). The average dilution seen in the data divided by that seen in Monte Carlo was found to be 0.96 ± 0.14. The distributions of $Q_\ell \cdot Q_{\rm B}$ are shown in Figure 2(d), again for events with $t_{\rm rec} < 2\,{\rm ps}$. Both Figures 2(c) and 2(d) show agreement between data and Monte Carlo.

The $Q_{\rm vtx}$, $Q^{\kappa=0.5}_{\rm opp}$ and $Q^{\kappa=0.4}_{\rm same}$ distributions are not necessarily charge symmetric because of detector effects causing a difference in the rate and reconstruction of positive and negative tracks. These effects are caused by the material in the detector and the Lorentz angle in the jet chamber. They were removed by subtracting offsets from the $Q_{\rm vtx}$, $Q^{\kappa=0.5}_{\rm opp}$ and $Q^{\kappa=0.4}_{\rm same}$ values before the $Q_{\rm B}$ tagging dilutions were calculated. The $Q_{\rm vtx}$ and $Q^{\kappa=0.5}_{\rm opp}$ offsets were determined using the inclusive lepton events selected from data. The $Q^{\kappa=0.4}_{\rm same}$ offset was determined from Monte Carlo B^0 jets, since no pure sample of fully reconstructed B^0 decays is available from the data. However, the $D^{*\pm}\ell$ events do allow this offset to be checked, even though some extra tracks may be present from D^{**} decays. The data and Monte Carlo were found to be in good agreement. The normalised offsets (the offsets divided by the r.m.s. widths) of the charge distributions were found to be $+0.029 \pm 0.011$, $+0.018 \pm 0.007$ and $+0.036 \pm 0.018$ for $Q_{\rm vtx}$, $Q^{\kappa=0.5}_{\rm opp}$ and $Q^{\kappa=0.4}_{\rm same}$ respectively. The error quoted for the $Q^{\kappa=0.4}_{\rm same}$ offset is the statistical precision of the $D^{*\pm}\ell$ events in data. If these offsets were not removed, they would induce respective shifts of -0.004, -0.003 and $+0.009$ in the overall $Q_{\rm B}$ distribution. If no corrections were applied for the offsets, the combined shift would be $+0.002$.

4 Fit and results

The reconstructed proper time $t_{\rm rec}$ and tagging variable $Q_{\rm B}$ of each of the 24 candidates is shown in Figure 3(a). The events with invariant mass in the range 5.15–5.40 GeV/c^2 are shown as filled circles, whilst the events in the ranges 5.00–5.15 and 5.40–5.60 GeV/c^2, which have lower signal purity, are shown as open circles.

In order to quantify the CP asymmetry in the data, an unbinned maximum likelihood fit was constructed, using four inputs for each $B^0 \to J/\psi K^0_S$ candidate: $t_{\rm rec}$, σ_t, $Q_{\rm B}$ and the event-by-event background probability $f_{\rm bac}$, derived from the mass and energy of each candidate (see Section 2). The total likelihood for an event was given by

$$\mathcal{L} = (1 - f_{\rm bac}) \cdot \mathcal{L}_{\rm sig} + f_{\rm bac} \cdot \mathcal{L}_{\rm bac} \; . \tag{9}$$

The signal likelihood $\mathcal{L}_{\rm sig}$ was defined as:

$$\mathcal{L}_{\rm sig}(t_{\rm rec}, \sigma_t, Q_{\rm B}; \sin 2\beta, \Delta m_{\rm d}, \tau^0) = \mathcal{F}_{\rm sig}(t) \otimes G(t - t_{\rm rec}, \sigma_t) \; , \tag{10}$$

where t is the true proper decay time, and $G(t - t_{\rm rec}, \sigma_t)$ is a Gaussian representing the proper decay time resolution. The true proper time distribution is given by

$$\mathcal{F}_{\rm sig}(t; \sin 2\beta, \Delta m_{\rm d}, \tau^0) = \frac{\exp(-t/\tau^0)}{\tau^0} \cdot (1 - Q_{\rm B} \sin 2\beta \sin \Delta m_{\rm d} t). \tag{11}$$

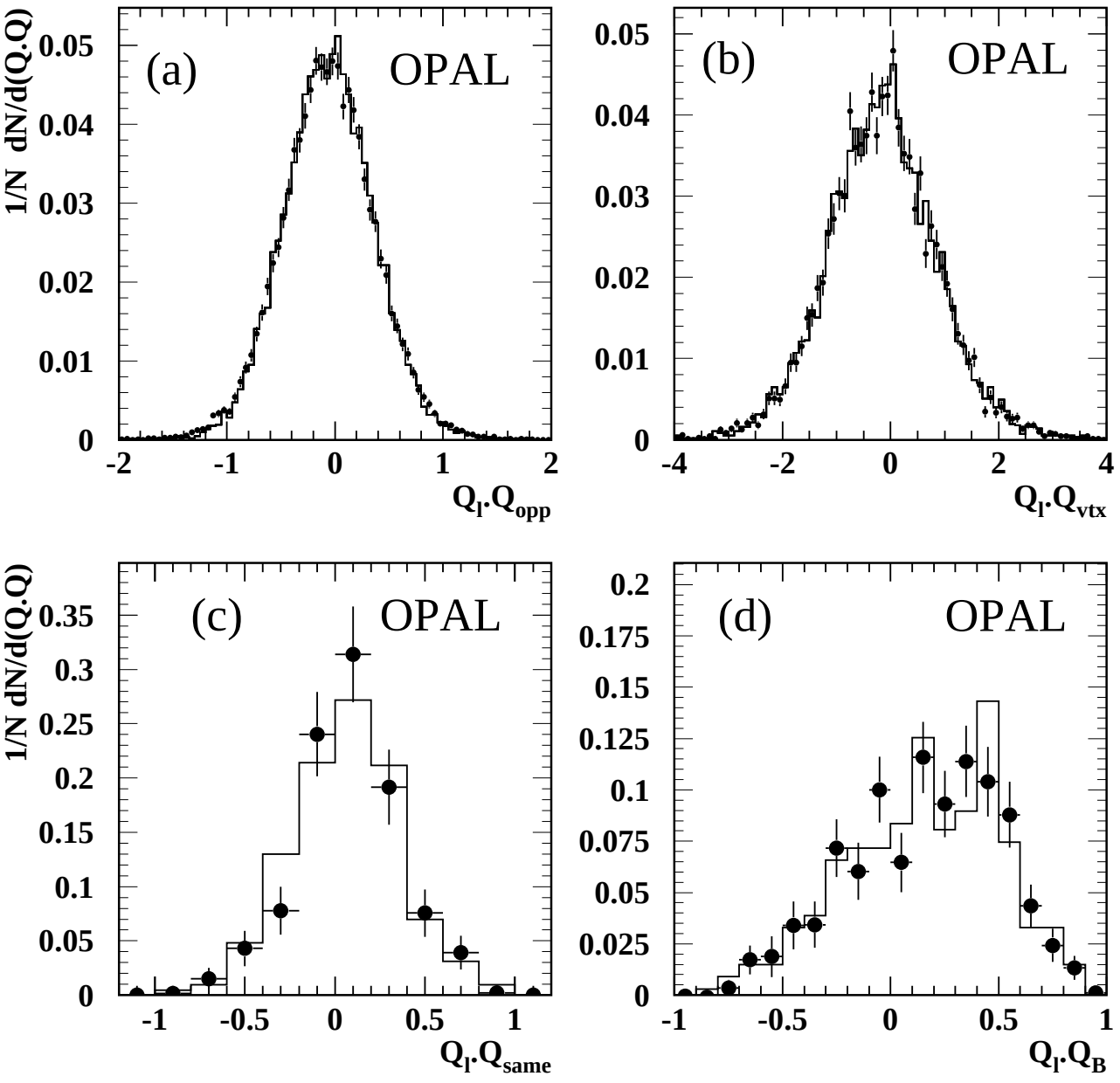

Figure 2: The distribution of the product of the lepton charge Q_ℓ and (a) the $Q_{\rm opp}^{\kappa=0.5}$ jet charge, (b) the $Q_{\rm vtx}$ vertex charge, (c) the $Q_{\rm same}^{\kappa=0.4}$ jet charge and (d) the $Q_{\rm B}$ tagging variable. Distributions (a) and (b) are taken from an inclusive lepton sample, whilst distributions (c) and (d) are taken from a $\mathrm{B}^0 \to \mathrm{D}^{*\pm}\ell$ sample, only including events with reconstructed proper time $t_{\rm rec} < 2\,$ps. The data are shown as points and the Monte Carlo predictions as histograms.

The B^0 lifetime, τ^0, was taken as 1.56 ± 0.06 ps [18], and Δm_d was taken as $0.467\pm0.022^{+0.017}_{-0.015}$ ps^{-1} [24]. The likelihood for the background, $\mathcal{L}_{bac}$, is defined in the same way, with the true proper time distribution:

$$\mathcal{F}_{bac}(t\ ;\tau_{bac}) = \frac{\exp(-t/\tau_{bac})}{\tau_{bac}}\ . \tag{12}$$

The background is dominated by $b\overline{b}$ events, and is assumed to have no CP asymmetry. Possible bias due to this assumption is treated as a systematic error. The effective background lifetime, τ_{bac}, was taken to be 2.0 ps from the Monte Carlo background sample. This value is larger than the average b lifetime of 1.55 ps [18] because the energy of the b hadron is systematically underestimated for the background events, since the tracks assigned to the $J/\psi K^0_S$ candidate do not, in general, include all the b-hadron decay products, and include fragmentation products. A large variation of ±0.4 ps in this parameter is considered in the systematic errors.

Fitting the data for the single parameter $\sin 2\beta$, gave the result

$$\sin 2\beta = 3.2^{+1.8}_{-2.0}\ .$$

The corresponding $\Delta \log \mathcal{L}$ distribution is shown in Figure 3(b). It can be parametrised as

$$\begin{aligned} -\Delta\log\mathcal{L} &= 0.116(\sin 2\beta - 3.2)^2 + 0.00224(\sin 2\beta - 3.2)^4 \qquad \sin 2\beta < 3.2 \\ -\Delta\log\mathcal{L} &= 0.125(\sin 2\beta - 3.2)^2 + 0.00985(\sin 2\beta - 3.2)^4 \qquad \sin 2\beta > 3.2\ . \end{aligned}$$

The parametrisation can be used to combine this result with future results from other experiments. To compare the fitted result with the data, an estimator, A, of the $B^0 \to J/\psi K^0_S$ asymmetry (corrected for the average dilution in each time bin) is shown in Figure 3(c) with the fit result superimposed, where

$$A = \frac{\sum (1 - f_{bac}) \cdot Q_B}{\sum (1 - f_{bac})^2 \cdot Q_B^2}\ , \tag{13}$$

and the summations are over all the events in a given time bin. The large observed values of A, typically exceeding the physical range of the asymmetry, are due to the tagging dilution factors and, to a lesser extent, the background fraction.

5 Systematic errors and cross checks

The main sources of systematic error and their effect on the measurement of $\sin 2\beta$ are listed in Table 1. The fit result is sensitive to the level and possible CP asymmetry of the background, the accuracy of the decay time reconstruction and the production flavour tagging dilution.

- The event-by-event purities of the 24 candidates have significant statistical errors from the background fit described in Section 2. The three fitted parameters (the number of signal candidates, the position of the B^0 mass peak and the Peterson parameter for the background energy distribution) were each varied by their statistical errors, one at a time, and the effect on $\sin 2\beta$ determined. As the correlations between these parameters were found to be less than 20%, these effects were added in quadrature, leading to a total error of $^{+0.06}_{-0.07}$ on $\sin 2\beta$.

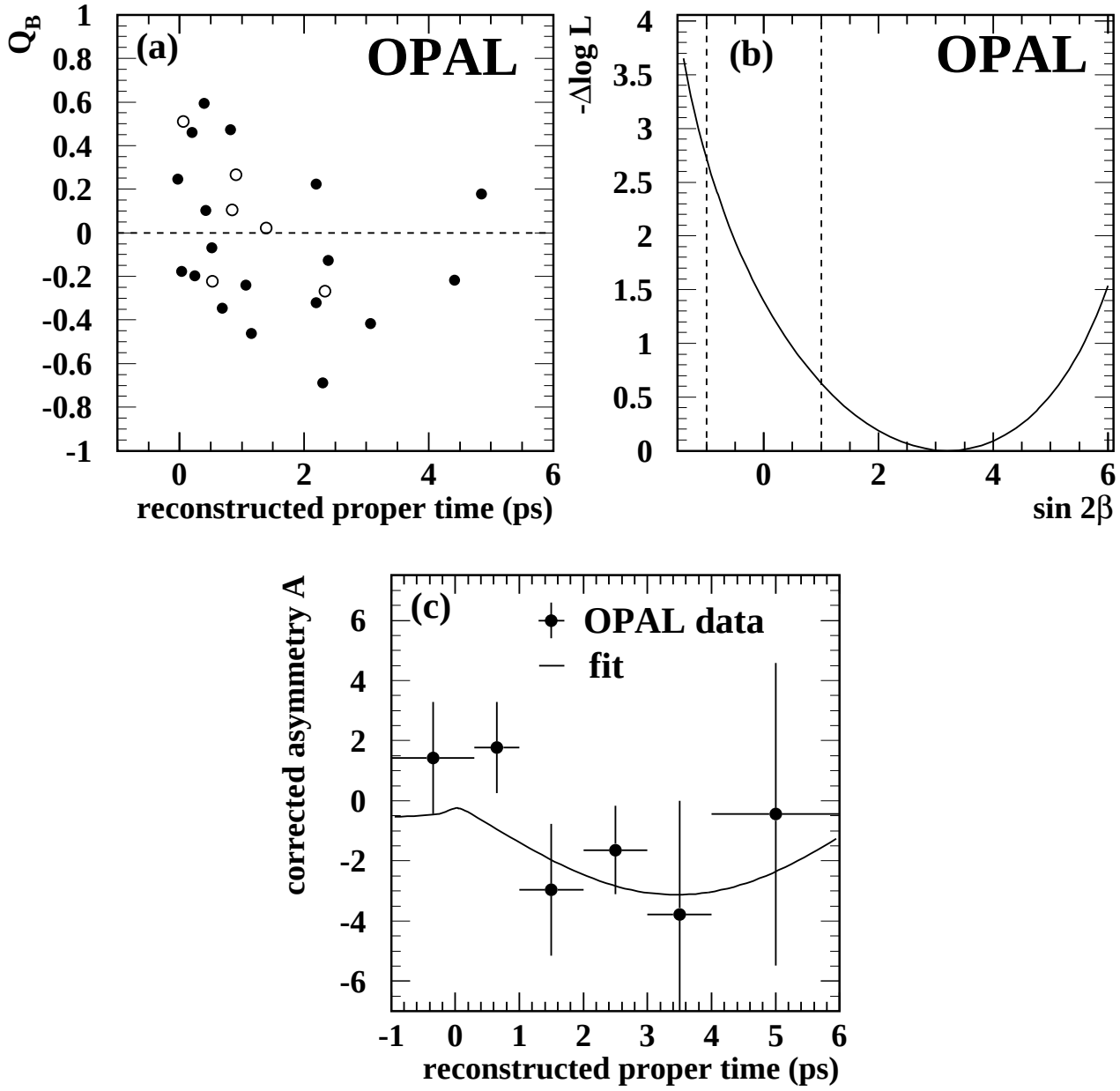

Figure 3: (a) The distribution of $Q_{\rm B}$ versus $t_{\rm rec}$ for the $\rm J/\psi K^0_S$ candidates with invariant masses in the range 5.15–5.40 GeV/c^2 (filled circles), and 5.00–5.15 GeV/c^2 and 5.40–5.60 GeV/c^2 (open circles); (b) the $-\Delta \log \mathcal{L}$ value as a function of $\sin 2\beta$ from the fit to the 24 data candidates, with the physical region indicated by the dotted lines; (c) the distribution of the corrected asymmetry, A, versus $t_{\rm rec}$ for the $\rm J/\psi K^0_S$ data, with the fit result superimposed.

- The background mass distribution is taken from a fit to a Monte Carlo sample with four times the statistics of the data sample. Various different parametrisations and the binned Monte Carlo distribution itself were tried. As an alternative method, the shape of the background was taken to be a falling exponential, with both the normalisation and decay constant of the background being fitted to the data, as in [8]. This fit predicts a signal purity of 52% compared to 60%. The Monte Carlo predicts a significant departure from the exponential shape due to decays of the type $\mathrm{B} \to \mathrm{J}/\psi \mathrm{K}^{(*)}\mathrm{X}$, followed by $\mathrm{K}^* \to \mathrm{K}^0_\mathrm{S}\pi$ when K^* are produced. Including this contribution explicitly and letting the fitted exponential describe the remaining background gives a purity of 53%. The data show a deficit of events in the region 4.7–4.9 GeV/c^2, possibly indicating that the Monte Carlo overestimates the background in this region. A further fit to the data alone was therefore performed, using only the data above 4.9 GeV/c^2, with the background described by a falling exponential, resulting in a signal purity of 73%. The largest variation in $\sin 2\beta$ resulting from these different parametrisations was found to be $^{+0.25}_{-0.32}$. An uncertainty of ± 0.32 was taken for the systematic error due to the background parametrisation.

- Uncertainty on the assumed mass and energy distributions for the signal also affects the result of the background fit. Monte Carlo events with tracking resolution degraded by 10% were used to parametrise the signal mass distribution, resulting in a shift in the fitted value of $\sin 2\beta$ of 0.07. The functional form used to fit the signal mass distribution was changed from three Gaussian functions to two, one for the peak of the distribution and another for the tail. This caused a shift of 0.11 on $\sin 2\beta$. The uncertainty on the B^0 energy distribution was assessed by varying the Peterson parameter ϵ to cause a change in the mean scaled energy of 0.02, larger than the uncertainty on the mean scaled energy of B hadrons [25]. The effect on $\sin 2\beta$ was negligible.

- The final state from the decay $\mathrm{B}^0 \to \mathrm{J}/\psi \mathrm{K}^{*0}$ followed by $\mathrm{K}^{*0} \to \mathrm{K}^0_\mathrm{S}\pi^0$ is expected to be mainly CP even (i.e. opposite CP to the $\mathrm{J}/\psi \mathrm{K}^0_\mathrm{S}$ final state), and so could give rise to a possible CP asymmetry in the background. The contribution from such decays in the signal region was estimated from Monte Carlo to be 0.7 events, and is indicated in Figure 1. If such a contribution had a maximal asymmetry, the effect on the fitted $\sin 2\beta$ would be 0.03. The contribution to the background CP asymmetry from B^0 decays involving K^0_L mesons was found to be negligible.

- The event-by-event proper time resolution σ_t is used in the likelihood fit. Monte Carlo studies indicate that the distribution of errors in reconstructed proper time divided by σ_t is well described by a Gaussian with zero mean and width 1.15 ± 0.15. If the proper time resolution is scaled by 1.3, the resulting change in $\sin 2\beta$ is 0.01.

- The description of $Q^{\kappa=0.5}_{\mathrm{opp}}$ and Q_{vtx} by the Monte Carlo was tested by comparing the correlation of these charges with the lepton charge in inclusive lepton events in data and Monte Carlo, as described in Section 3. The uncertainty on the Q_B values was assessed by scaling the $Q^{\kappa=0.5}_{\mathrm{opp}}$ and Q_{vtx} values independently by 1.16 and 1.12, respectively. These scalings correspond to the sum in quadrature of the differences seen between data and Monte Carlo and the statistical precision of the comparisons. The uncertainty on the modelling of $Q^{\kappa=0.4}_{\mathrm{same}}$ was assessed using $\mathrm{D}^{*\pm}\ell$ data as described in Section 3. The systematic uncertainty was determined by scaling the values of $Q^{\kappa=0.4}_{\mathrm{same}}$ by 1.2, again corresponding to the quadrature sum of the difference seen between data and Monte Carlo and the

Source	$\delta(\sin 2\beta)$
Background level (data statistics)	$^{+0.06}_{-0.07}$
Background shape	± 0.32
Signal shape	± 0.13
Background asymmetry	± 0.03
Proper time reconstruction	± 0.01
Jet and vertex charge modelling	$^{+0.31}_{-0.26}$
Jet charge offsets	$^{+0.14}_{-0.08}$
Vertex charge performance	± 0.01
$\Delta m_{\rm d}$ value	± 0.10
$\rm B^0$ lifetime	± 0.01
Background lifetime (± 0.4 ps)	$^{+0.01}_{-0.02}$
Total	$^{+0.50}_{-0.46}$

Table 1: Sources of systematic error in the measurement of $\sin 2\beta$.

statistical precision of the comparison. The total systematic error on $\sin 2\beta$ from these effects is $^{+0.31}_{-0.26}$.

- The offsets applied to $Q_{\rm vtx}$ and $Q^{\kappa=0.5}_{\rm opp}$ were determined from data as described in Section 3. These were varied by their statistical uncertainties. The offset to the $Q^{\kappa=0.4}_{\rm same}$ jet charge was determined from Monte Carlo, and checked using the $\rm B^0 \to D^{*\pm}\ell$ candidates. The offset was varied by the statistical precision of this test. The effect of these variations results in changes in $\sin 2\beta$ of $^{+0.14}_{-0.08}$.

- The performance of the vertex charge algorithm is sensitive to the tracking resolution. The Monte Carlo has been tuned to reproduce the data impact parameter resolutions as a function of $\cos\theta$, p and the different sub-detectors contributing to a track measurement. Residual uncertainties were estimated by degrading the resolution of all tracks by 10% using a simple smearing technique. The neural network training and mistag parametrisations were repeated on this degraded sample, which was then used to derive the $Q_{\rm B}$ values that enter the fit for $\sin 2\beta$. The resulting change in $\sin 2\beta$ was 0.01.

- The values for $\Delta m_{\rm d}$ and the $\rm B^0$ lifetime were varied within their errors to give the uncertainties listed in the table. The value of $\tau_{\rm bac}$ was varied by a conservative 0.4 ps (the difference between the predicted Monte Carlo background lifetime and the average B meson lifetime) to allow for uncertainties on the B energy mismeasurement.

The total systematic error is thus ± 0.5. Many of the sources of error have a statistical component, and many of them scale with the fitted value of $\sin 2\beta$. The systematic error would thus decrease in an analysis with higher statistics.

A number of consistency checks were also performed. The result was found to be stable when the least well tagged events (those with $|Q_{\rm B}| < 0.25$), the events with highest background ($f_{\rm bac} > 0.5$), or the events outside the purest mass region (5.15–5.40 $\rm GeV/c^2$) were removed.

The values of $\sin 2\beta$ resulting from these checks were found to be $4.0^{+1.9}_{-2.3}$, $3.2^{+1.8}_{-2.0}$ and $2.8^{+1.9}_{-2.0}$ respectively. The data were fitted for the B^0 lifetime, giving a result of $1.2^{+0.5}_{-0.4}$ ps (independent of $\sin 2\beta$), consistent with the world average. In addition, the assumption that the background exhibits no CP asymmetry was tested by repeating the fit, using only events in the sideband region and setting $f_{\rm bac}$ to 0 for every event. The fitted value of $\sin 2\beta$ in this case was $0.38^{+0.45}_{-0.49}$, consistent with zero. The selection cuts were loosened to give a sideband data sample three times larger, and a fitted value of $\sin 2\beta$ of -0.12 ± 0.30 was obtained. The background and CP asymmetry fits were also repeated on a Monte Carlo sample with no CP violation and four times the data statistics, giving asymmetries consistent with zero for both signal and sideband regions. The $B^0 \to D^{*\pm}\ell$ sample was used to perform a further cross check for the absence of large biases in the determination of $Q_{\rm B}$. The events were separated according to the sign of Q_ℓ, and the average $Q_{\rm B}$, $\langle Q_{\rm B}^+ \rangle$ and $\langle Q_{\rm B}^- \rangle$, was calculated for each subsample. To account for charge biases due to the $D^{*\pm}$ selection, the average value of $Q_{\rm B}$ was calculated as $(\langle Q_{\rm B}^+ \rangle + \langle Q_{\rm B}^- \rangle)/2$ and was found to be -0.016 ± 0.011, consistent with zero. The Monte Carlo prediction for the $Q_{\rm opp}^{\kappa=0.5}$ offset, which is not used in the analysis, disagrees with the value determined from the data. If the fit is repeated taking all offsets from the Monte Carlo, $\sin 2\beta$ is shifted by -0.28. This discrepancy between data and Monte Carlo does not affect the description of the tagging dilution.

The value of $\sin 2\beta$ can also be estimated from the time-integrated asymmetry. In this case, the lower limit of the time integration can be varied to optimise the sensitivity — i.e. the ability to distinguish different true values of $\sin 2\beta$. For data samples of this size and purity, the optimum lower bound[5] was found, using Monte Carlo studies, to be 0.7 ps. The value of $\sin 2\beta$ obtained from our data sample using this method is $2.0^{+1.1}_{-1.5}$, where 12 events are included in the range of integration. The probability of obtaining time dependent and time integrated measurements disagreeing at this level or more was found to be 20%. Monte Carlo studies indicate that the errors obtained from both types of fit increase as the central values deviate from zero, and that the time dependent fit yields smaller errors on average. They also show that the time dependent fit has a greater sensitivity to the true value of $\sin 2\beta$ than the time integrated method, even after optimising the lower time-integration bound.

6 Discussion and conclusion

The result from this analysis can be interpreted by calculating the probabilities to see a deviation, in the positive $\sin 2\beta$ direction, at least as far from the true value as that observed, for different true values of $\sin 2\beta$. The deviation is defined by the difference in $\log \mathcal{L}$ between the fitted value and the assumed true value. This definition is used because the sensitivity varies from experiment to experiment. Monte Carlo samples of 24 candidates, with the same background and tagging distributions as those expected in the data, were generated to determine these probabilities. The probabilities for the $\log \mathcal{L}$ differences seen in the data, with correction for the systematic error, were found to be be 1.6%, 7.8% and 21.3% if the true value of $\sin 2\beta$ were -1, 0 and $+1$, respectively. These probabilities indicate the consistency of the result with these values of $\sin 2\beta$, and should not be interpreted as confidence levels. The distributions of fitted $\sin 2\beta$ for Monte Carlo experiments with true $\sin 2\beta$ of -1, 0 and $+1$ are shown in

[5] The value is smaller than that which would be obtained in the absence of background.

Figures 4(a), (b) and (c).

An alternative interpretation is given by the Bayesian approach [26] assuming equal *a priori* probabilities for every possible true value of $\sin 2\beta$. In this case, the probabilities for $\sin 2\beta$ to be greater or less than zero, with correction for the systematic error, are found to be 68.5% and 31.5% respectively.

In conclusion, the time dependent CP asymmetry in the decays $B^0 \to J/\psi K^0_S$ and $\bar{B}^0 \to J/\psi K^0_S$ has been measured using data collected with the OPAL detector at LEP between 1990 and 1995. From 24 reconstructed $B^0 \to J/\psi K^0_S$ candidates with a purity of about 60%, the CP violation amplitude, which is $\sin 2\beta$ in the Standard Model, has been found to be:

$$\sin 2\beta = 3.2^{+1.8}_{-2.0} \pm 0.5 \ ,$$

where the first error is statistical and the second systematic. The systematic error has a large statistical component, and much of it scales with the central value.

This is the first direct study of the CP asymmetry in the $B^0 \to J/\psi K^0_S$ system. It can be combined with other results in the future by using the log-likelihood curve given in section 4.

Acknowledgements

We particularly wish to thank the SL Division for the efficient operation of the LEP accelerator at all energies and for their continuing close cooperation with our experimental group. We thank our colleagues from CEA, DAPNIA/SPP, CE-Saclay for their efforts over the years on the time-of-flight and trigger systems which we continue to use. In addition to the support staff at our own institutions we are pleased to acknowledge the
Department of Energy, USA,
National Science Foundation, USA,
Particle Physics and Astronomy Research Council, UK,
Natural Sciences and Engineering Research Council, Canada,
Israel Science Foundation, administered by the Israel Academy of Science and Humanities,
Minerva Gesellschaft,
Benoziyo Center for High Energy Physics,
Japanese Ministry of Education, Science and Culture (the Monbusho) and a grant under the Monbusho International Science Research Program,
German Israeli Bi-national Science Foundation (GIF),
Bundesministerium für Bildung, Wissenschaft, Forschung und Technologie, Germany,
National Research Council of Canada,
Research Corporation, USA,
Hungarian Foundation for Scientific Research, OTKA T-016660, T023793 and OTKA F-023259.

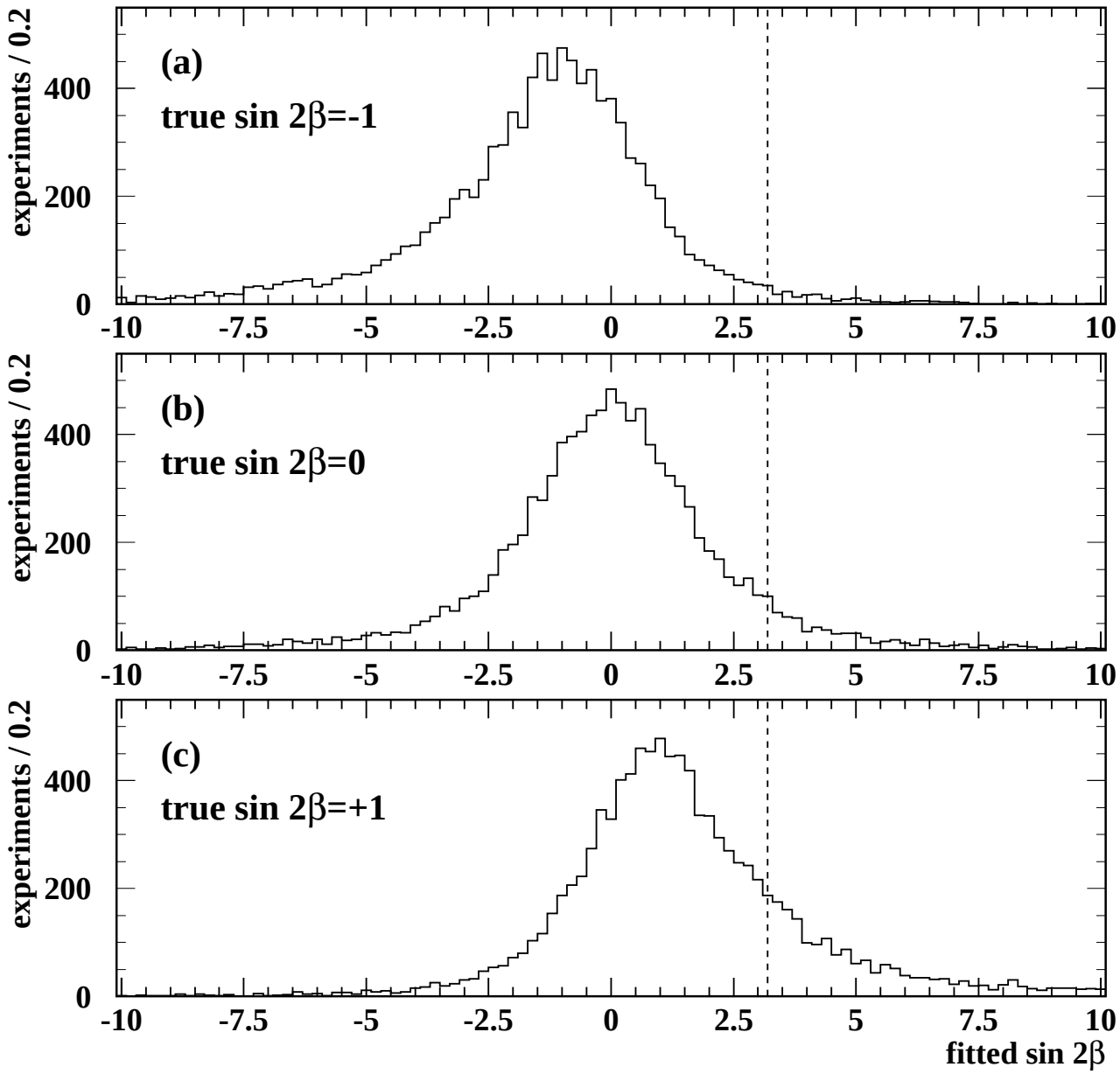

Figure 4: The distributions of fitted $\sin 2\beta$ in Monte Carlo samples of 24 events. The dotted lines indicate the data fitted value.

References

[1] J.H. Christenson, J.W. Cronin, V.L. Fitch and R. Turlay, Phys. Rev. Lett. **13** (1964) 138.

[2] For recent reviews see :
M. Neubert, Int. J. Mod. Phys. **A 11** (1996) 4173, hep-ph/9604412;
A. Ali and D. London, Nucl. Phys. Proc. Suppl. **54 A** (1997) 297, hep-ph/9607392;
A.J. Buras and R. Fleischer, hep-ph/9704376, to appear in Heavy Flavours II, World Scientific (1997), eds. A.J. Buras and M. Linder;
Y. Nir, hep-ph/9709301, to appear in the Proceedings of the 18th International Symposium on Lepton Photon Interactions Hamburg, Germany, July 28 - August 1 1997;
I. Dunietz, Fermilab-CONF-97/278-T, hep-ph/9709448.

[3] CLEO Collaboration, J. Bartelt *et al.*, Phys. Rev. Lett. **71** (1993) 1680;
CDF Collaboration, F. Abe *et al.*, Phys. Rev. **D 55** (1997) 2546.

[4] OPAL Collaboration, K. Ackerstaff *et al.*, Z. Phys. **C 76** (1997) 401.

[5] I.I. Bigi and A.I. Sanda, Nucl. Phys. **B 193** (1981) 85.

[6] L. Wolfenstein, Phys. Rev. Lett. **13** (1964) 562.

[7] OPAL Collaboration, K. Ahmet *et al.*, Nucl. Inst. and Meth. **A 305** (1991) 275;
P. Allport *et al.*, Nucl. Inst. and Meth. **A 324** (1993) 34;
P. Allport *et al.*, Nucl. Inst. and Meth. **A 346** (1994) 476.

[8] OPAL Collaboration, G. Alexander *et al.*, Z. Phys. **C 70** (1996) 197.

[9] T. Sjöstrand, Comp. Phys. Comm. **39** (1986) 347;
M. Bengtsson and T. Sjöstrand, Comp. Phys. Comm. **43** (1987) 367;
M. Bengtsson and T. Sjöstrand, Nucl. Phys. **B 289** (1987) 810;
T. Sjöstrand, CERN-TH/6488-92.
Parameter values were tuned to describe global event shape variables, inclusive particle yields and fragmentation functions:
OPAL Collaboration, G. Alexander *et al.*, Z. Phys. **C 69** (1996) 543.

[10] J. Allison *et al.*, Nucl. Instrum. Methods **A 317** (1992) 47.

[11] OPAL Collaboration, R. Akers *et al.*, Phys. Lett. **B 327** (1994) 411.

[12] OPAL Collaboration, R. Akers *et al.*, Z. Phys. **C 70** (1996) 357.

[13] The variable $E_{\rm cone}$ is called $E_{\rm cone2}$ in the reference:
OPAL Collaboration, P.D. Acton *et al.*, Z. Phys. **C 55** (1992) 191.

[14] O. Dahl *et al.*, The SQUAW package, LBL Group A, Programming note P-126 (1968).

[15] OPAL Collaboration, P.D. Acton *et al.*, Phys. Lett. **B 298** (1993) 456.

[16] OPAL Collaboration, P.D. Acton *et al.*, Z. Phys. **C 59** (1993) 183;
OPAL Collaboration, R. Akers *et al.*, Phys. Lett. **B 338** (1994) 497.

[17] C. Peterson, D. Schlatter, I. Schmitt and P. Zerwas, Phys. Rev. **D 27** (1983) 105.

[18] Particle Data Group, M. Aguilar-Benitez *et al.*, Phys. Rev. **D 54** (1996) 1.

[19] JADE Collaboration, W. Bartel *et al.*, Z. Phys. **C 33** (1986) 23;
JADE Collaboration, S. Bethke *et al.*, Phys. Lett. **B 213** (1988) 235.

[20] OPAL Collaboration, R. Akers *et al.*, Z. Phys. **C 65** (1995) 17.

[21] OPAL Collaboration, K. Ackerstaff *et al.*, CERN-PPE/97-115, to be published in Eur. Phys. J. C.

[22] OPAL Collaboration, R. Akers *et al.*, Z. Phys. **C 66** (1995) 19.

[23] OPAL Collaboration, K. Ackerstaff *et al.*, Phys. Lett. **B 395** (1997) 128.

[24] OPAL Collaboration, K. Ackerstaff *et al.*, Z. Phys. **C 76** (1997) 417.

[25] ALEPH Collaboration, D. Buskulic *et al.*, Phys. Lett. **B 357** (1995) 699;
ALEPH Collaboration, D. Buskulic *et al.*, Z. Phys. **C 62** (1994) 179;
DELPHI Collaboration, P. Abreu *et al.*, Z. Phys. **C 66** (1995) 323;
OPAL Collaboration, G. Alexander *et al.*, Phys. Lett. **B 364** (1995) 93.

[26] F.T. Solmitz, Ann. Rev. Nucl. Sci. **14** (1964) 375.

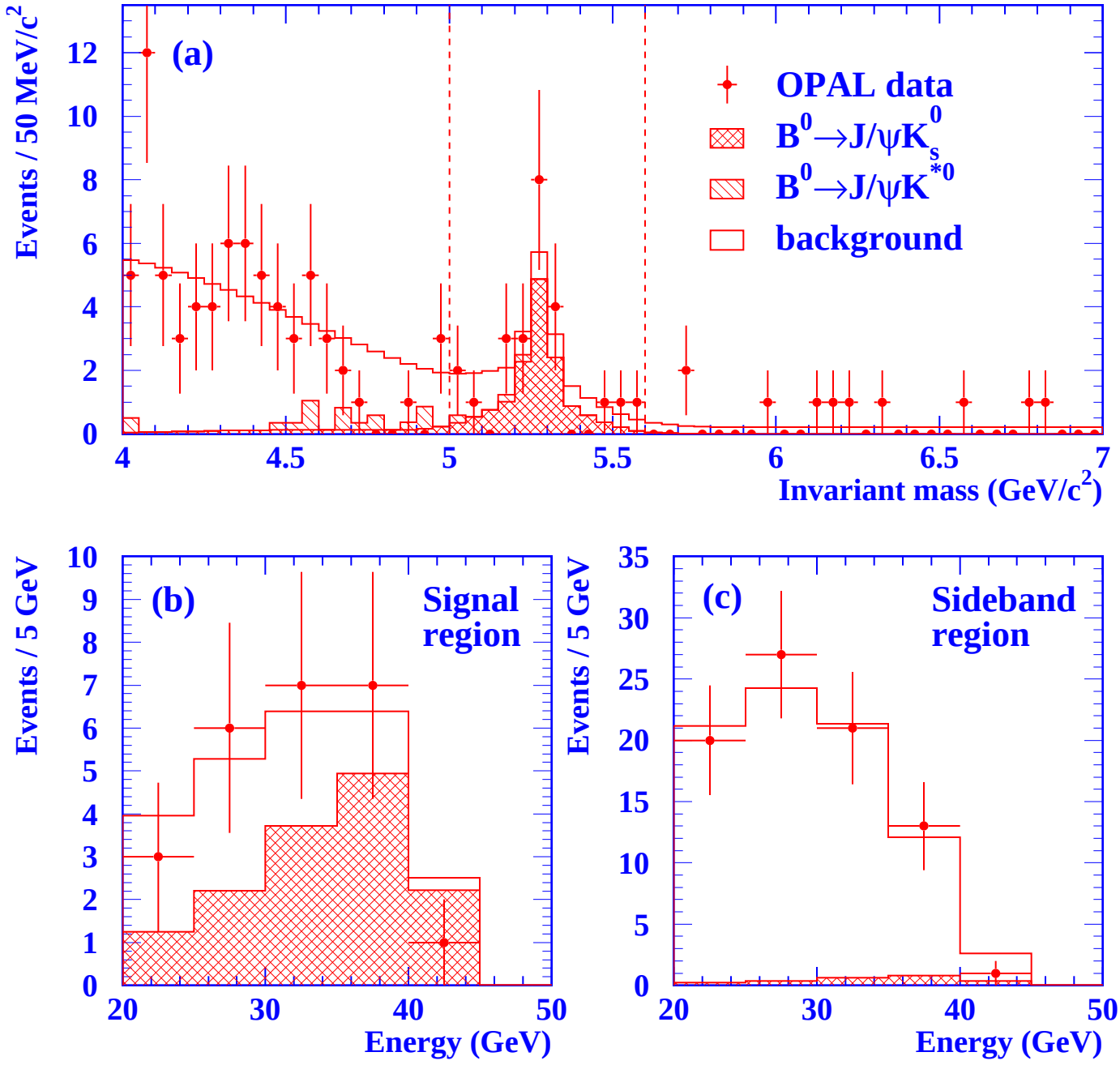
(a)
OPAL data
$B^0 \to J/\psi K^0_s$
$B^0 \to J/\psi K^{*0}$
background
Events / 50 MeV/c^2
Invariant mass (GeV/c^2)
(b)
Signal region
Events / 5 GeV
Energy (GeV)
(c)
Sideband region
Events / 5 GeV
Energy (GeV)

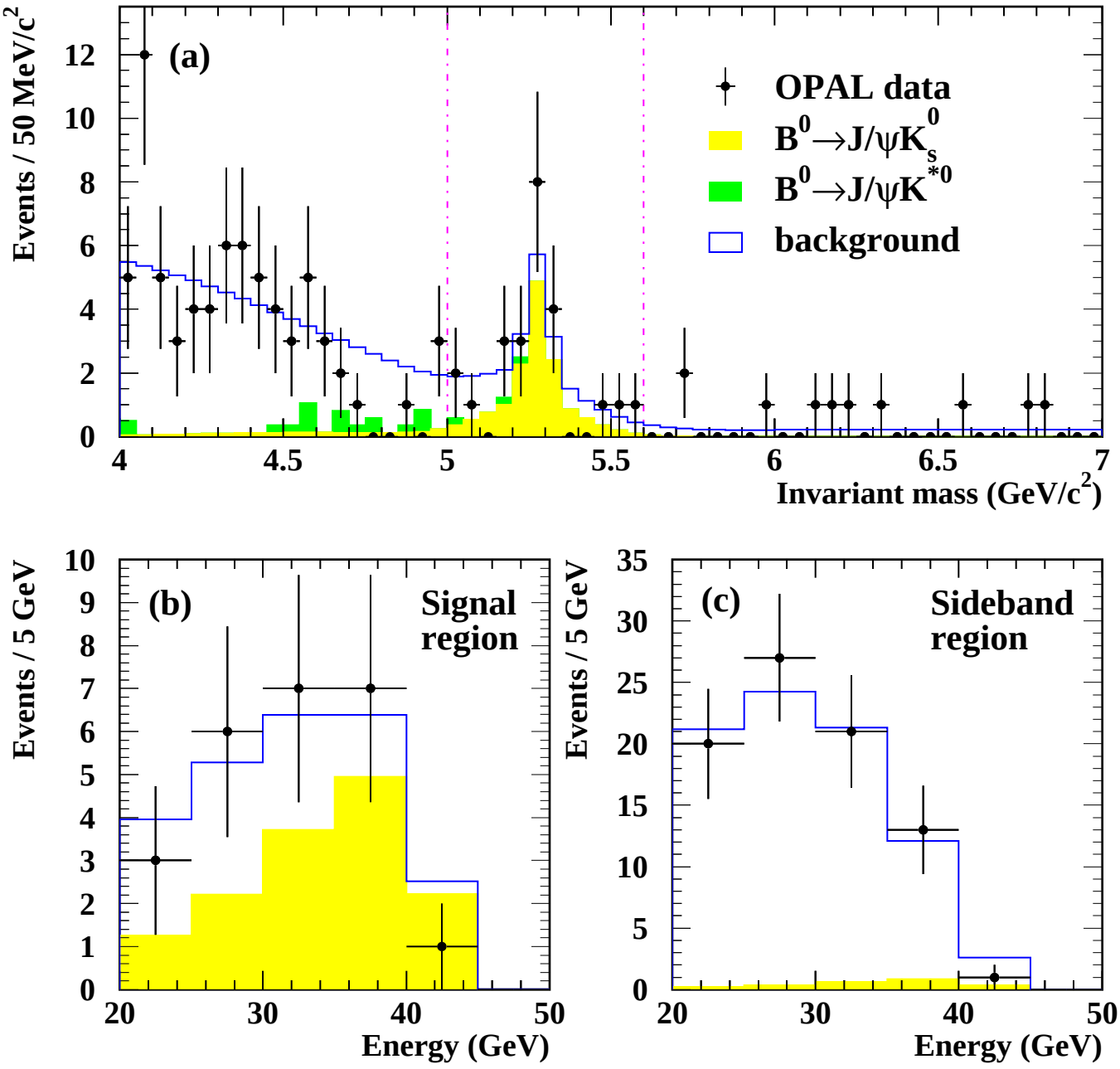
(a)
OPAL data
$B^0 \to J/\psi K_s^0$
$B^0 \to J/\psi K^{*0}$
background
Events / 50 MeV/c^2
Invariant mass (GeV/c^2)
(b)
Signal region
Events / 5 GeV
Energy (GeV)
(c)
Sideband region
Events / 5 GeV
Energy (GeV)

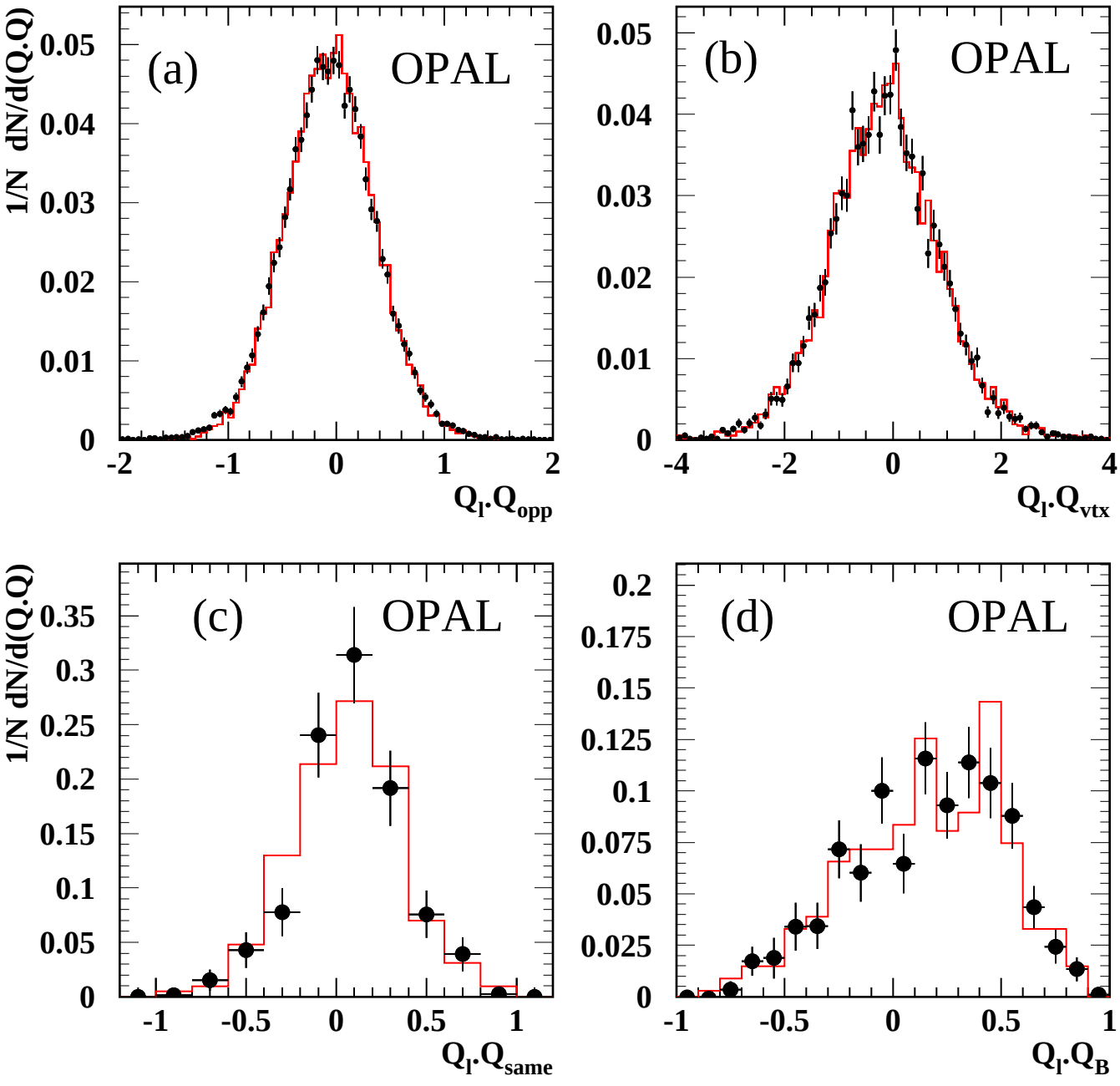
(a)
OPAL
1/N dN/d(Q.Q)
0.05
0.04
0.03
0.02
0.01
0
-2
-1
0
1
2
$Q_l.Q_{opp}$
(b)
OPAL
0.05
0.04
0.03
0.02
0.01
0
-4
-2
0
2
4
$Q_l.Q_{vtx}$
(c)
OPAL
1/N dN/d(Q.Q)
0.35
0.3
0.25
0.2
0.15
0.1
0.05
0
-1
-0.5
0
0.5
1
$Q_l.Q_{same}$
(d)
OPAL
0.2
0.175
0.15
0.125
0.1
0.075
0.05
0.025
0
-1
-0.5
0
0.5
1
$Q_l.Q_B$

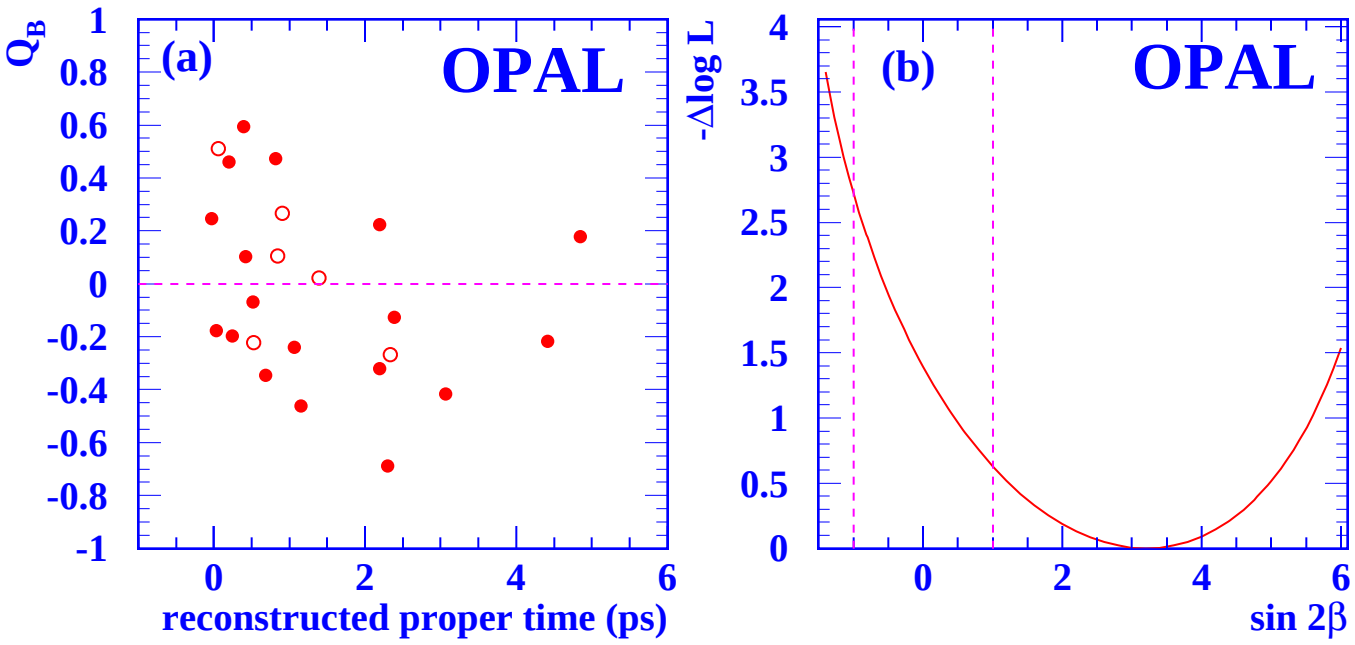
(a)
OPAL
Q_B
reconstructed proper time (ps)
(b)
OPAL
-Δlog L
sin 2β

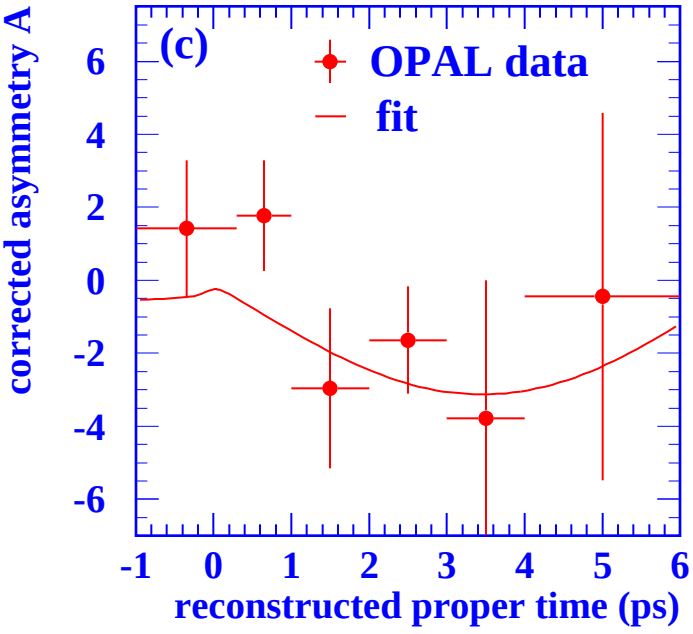
(c)
OPAL data
fit
corrected asymmetry A
reconstructed proper time (ps)

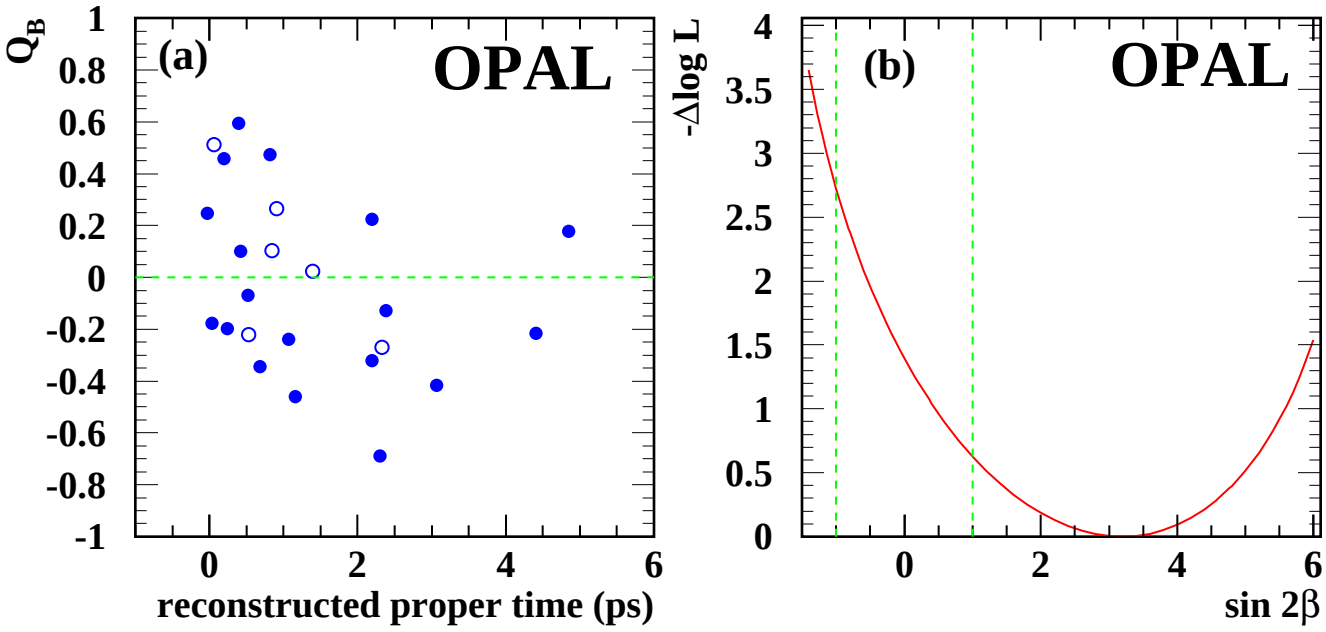
(a)
OPAL
Q_B
reconstructed proper time (ps)
(b)
OPAL
-Δlog L
sin 2β

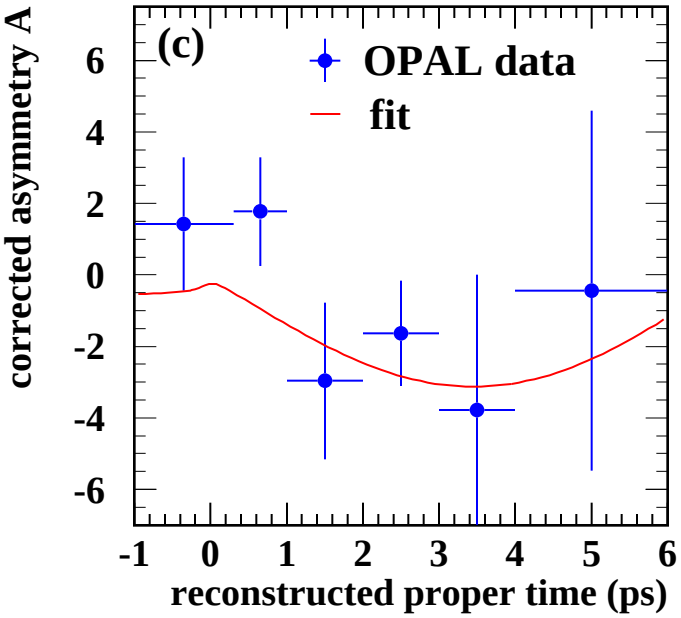
(c)
OPAL data
fit
corrected asymmetry A
reconstructed proper time (ps)

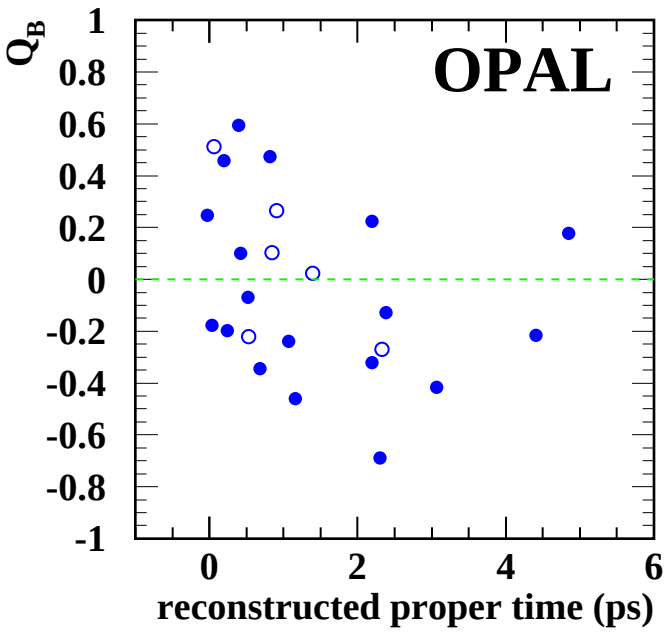
OPAL
Q_B
1
0.8
0.6
0.4
0.2
0
-0.2
-0.4
-0.6
-0.8
-1
0
2
4
6
reconstructed proper time (ps)

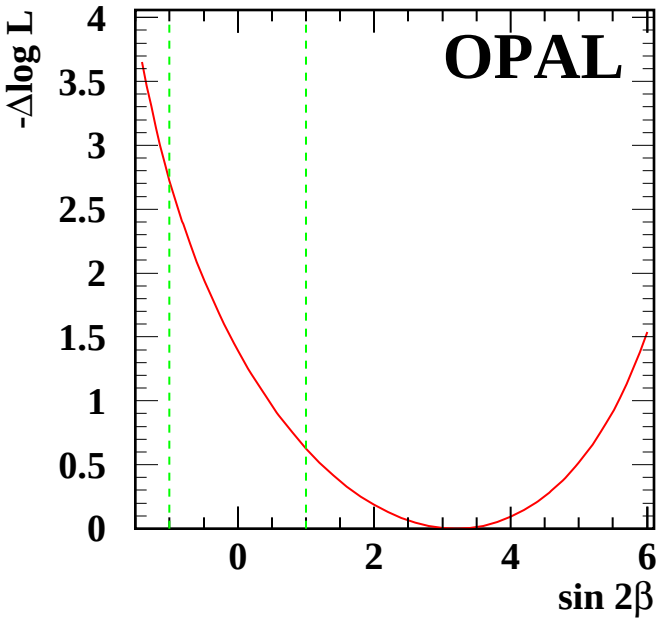
OPAL
-Δlog L
4
3.5
3
2.5
2
1.5
1
0.5
0
0
2
4
6
sin 2β

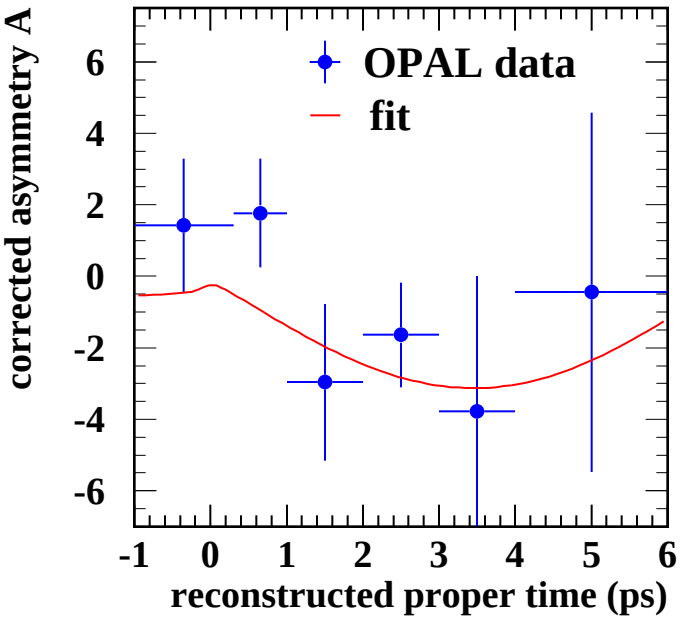
corrected asymmetry A
6
4
2
0
-2
-4
-6
-1
0
1
2
3
4
5
6
reconstructed proper time (ps)
OPAL data
fit